

The synthesis of Ag_3PO_4 under graphene oxide and hydroxyapatite aqueous dispersion for enhanced photocatalytic activity

by Admin Publikasi

Submission date: 27-Mar-2022 05:52AM (UTC+0700)

Submission ID: 1793620432

File name: IOP_Conf_Ser_Earth_Environ-The_synthesis_of_kompres.pdf (410.1K)

Word count: 3585

Character count: 18811

PAPER • OPEN ACCESS

The synthesis of Ag_3PO_4 under graphene oxide and hydroxyapatite aqueous dispersion for enhanced photocatalytic activity

5

To cite this article: U Sulaeman *et al* 2021 *IOP Conf. Ser.: Earth Environ. Sci.* **746** 012040

View the [article online](#) for updates and enhancements.

The synthesis of Ag_3PO_4 under graphene oxide and hydroxyapatite aqueous dispersion for enhanced photocatalytic activity

4
U Sulaeman*, R D Permadi, H Diastuti

Department of Chemistry, Jenderal Soedirman University, Purwokerto, 53123
Indonesia

*Email: sulaeman@unsoed.ac.id

Abstract. The development of Ag_3PO_4 photocatalyst for organic pollutant degradation is very challenging due to excellent activity under visible light exposure. The research aims to synthesize Ag_3PO_4 under graphene oxide (GO) and hydroxyapatite (HA) as a phosphate ion source for Rhodamin B degradation. The $\text{Ag}_3\text{PO}_4/\text{GO}$ was prepared using the precipitation method with the starting material of graphene oxide aqueous dispersion, AgNO_3 , and hydroxyapatite suspension. The structure, absorption, morphology, and element composition of photocatalysts were studied using XRD, DRS, SEM, and EDX. Photocatalytic abilities of the samples were tested using RhB oxidation under blue light exposure. The results exhibited that GO improves the crystallinity and visible absorption spectrum of Ag_3PO_4 . Incorporating GO on Ag_3PO_4 decreases the ratio of O/Ag and O/P leading to a defect formation. The reaction mechanism on the surface of the photocatalyst was mainly run by holes and superoxide radical ions. The modification of Ag_3PO_4 using hydroxyapatite and GO improved photocatalytic activity.

1. Introduction

Recently, the utilization of graphene oxide (GO) on the synthesis of silver phosphate-based photocatalyst has greatly developed. This modification has significantly improved the performance of photocatalysts. GO has potential applications due to good thermal stability, flame resistance, and mechanical performance [1]. The application of GO on Ag_3PO_4 can increase adsorption performance [2,3], expand the visible light absorption [4,5], enhance the photogenerated charge separation efficiency [6–8], and improve the charge collection efficiency [9]. The immobilization of $\text{Ag}_3\text{PO}_4/\text{GO}$ composite on the nickel foam improves the adsorption ability [2]. This design bringing the photogenerated electrons is highly transferred away, leading to a stable and efficient photocatalyst. The design of $\text{Ag}_3\text{PO}_4/\text{graphene oxide}$ aerogel composites using the hydrothermal method increases the specific surface area that improves the adsorption performance [3]. The incorporation of GO into Ag_3PO_4 can influence the absorption properties, such as redshift absorption [5]. GO can improve both the visible region's absorption and adsorption properties after coupling with Ag_3PO_4 [4]. GO is also a good electron acceptor that can capture photoexcited electrons and enhance the electron transfer and charge separation [6]. In the composite of $\text{ZnO}/\text{GO}/\text{Ag}_3\text{PO}_4$, GO can act as a bridge between ZnO and Ag_3PO_4 that can increase the transmission rate [7]. This composite showed higher adsorption, a more effective separation of hole and electron, and a higher rate of electron transfer. This phenomenon was

also found in GO-Ag₃PO₄/Bi₂O₃, GO can serve as a facilitator to transfer the photoexcited electrons from the CB (conduction band) of Bi₂O₃ to the VB (valence band) of Ag₃PO₄, generating the Z-scheme reaction [8].

The improvement of Ag₃PO₄ photocatalyst can also be supported by hydroxyapatite (HA). The Ag₃PO₄/HA composite design generated a redshift and high absorption in visible and UV regions that lead to improved catalytic properties [10]. The catalytic improvement was also provided through a synergistic effect of HA, carbon dots, and Ag₃PO₄ as found in the composite of HA/N-doped carbon dots/Ag₃PO₄ [11]. This modification successfully increased active sites. Coupling the Ag₃PO₄ and HA enhanced catalytic performance through a vacancy of HA that was created under irradiation leading to a Z-scheme reaction [12]. Ag₃PO₄/HA composites can also have adsorption properties for Pb(II) [13]. This phenomenon could be applied for Pb(II) immobilization, which was very beneficial for water treatment. Interestingly the HA can be utilized as a phosphate source of Ag₃PO₄ [14]. This preparation successfully enhances the absorption spectrum in the visible region, decreases the particle size, and changes the mechanism of active species.

Based on the above reports, coupling GO on Ag₃PO₄ using hydroxyapatite is very promising. The GO can improve the separation of photoexcited electrons and holes, and hydroxyapatite can enhance absorption in the visible region. The experiment aims to incorporate the graphene oxide on Ag₃PO₄ that is synthesized under hydroxyapatite suspension. This method is new in the application of GO and hydroxyapatite for Ag₃PO₄ preparation. It has not yet been reported by other researchers. The results showed that the simultaneous design using GO and hydroxyapatite increased the crystallinity and visible absorption of Ag₃PO₄. This modification might induce defect formation in Ag₃PO₄. These phenomena improve the efficiency of separation of hole and electron, leading to high catalytic activity.

2. Materials and Methods

2.1. Materials

The materials of AgNO₃ (Merck), CaCl₂ (Merck), KH₂PO₄ (Merck), ethylenediamine (Merck), and graphene oxide aqueous dispersion (5 mg/mL) (Goographene, USA), were used in the synthesis of the photocatalyst. The Rhodamine B (Merck) was used as a dye for the analysis of photocatalytic activity.

2.2. Synthesis

The Ag₃PO₄/GO was synthesized using the starting material of AgNO₃, graphene oxide aqueous dispersion, and hydroxyapatite (Ca₁₀(PO₄)₆(OH)₂) as a source of silver and phosphate respectively. The hydroxyapatite (HA) was synthesized using CaCl₂ and KH₂PO₄ at pH 8 adjusted using ethylenediamine [14,15]. The co-precipitation method was applied to prepare the photocatalyst of Ag₃PO₄/GO. The quantity of 0.45 g of graphene oxide aqueous dispersion (5 mg/mL) was added to the AgNO₃ solution (1 g of AgNO₃ in 10 mL of water). This mixture was added to the hydroxyapatite suspension (0.3 g of HA in 20 mL of water), mixed under a magnetic stirrer for 30 minutes. The precipitates were filtered, washed with water three times, and dried at 105°C for 5 hours. The Ag₃PO₄ without graphene oxide was also prepared with a similar procedure.

2.3. Characterization

The structure of Ag₃PO₄ and Ag₃PO₄/GO were characterized using the XRD (Rigaku Miniflex 600), operating at 40 kW, 15 mA, using Cu. The morphology and atomic composition were analyzed using SEM-EDX (JEOL, JSM-6510). The morphology magnification of 15000 times was set at 20 kV. The composition was analyzed using ZAF Method Standardless Quantitative Analysis at 20 kV, with a magnification of 3000 times, a counting rate of 3232 cps, and an energy range of 0-20 keV. Absorptions were analyzed using UV-vis DRS (JASCO V-670) with a wavelength range of 320-700 nm.

2.4. Photocatalytic Activity

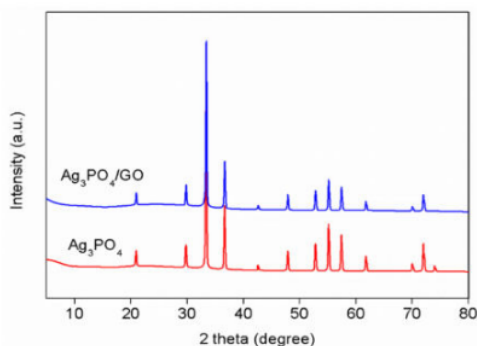
The photocatalytic ability of Ag_3PO_4 and $\text{Ag}_3\text{PO}_4/\text{GO}$ were examined using RhB oxidation under the blue LED lamp (Duralux, 3 Watt) [14,16]. The catalyst (0.1 g) was mixed with RhB solution (100 mL, 10 mg/L). The dark treatment and photocatalytic reactions were set at 10 and 8 minutes, respectively. The solution (5 ml) was taken out every 2 minutes and separated from the catalyst using centrifugation. The RhB concentration was monitored by the spectrophotometer. The catalytic recyclability was evaluated up to 3 cycles of 1st, 2nd, and 3rd reactions.

3. Results and Discussion

The Ag_3PO_4 was successfully designed using AgNO_3 , hydroxyapatite, and graphene oxide. The body-centered cubic structure was created in both Ag_3PO_4 and $\text{Ag}_3\text{PO}_4/\text{GO}$ (JCPDS No. 06-0505) [17] (figure 1). Figure 2 showed the absorption of Ag_3PO_4 and $\text{Ag}_3\text{PO}_4/\text{GO}$ at 320-700 nm. The broad absorption above 520 nm was observed in $\text{Ag}_3\text{PO}_4/\text{GO}$. This phenomenon might be originated from the formation of the defect site. The absorption coefficient and the band-gap can follow the direct transition of Tauc's relation [18,19]:

$$(\alpha h\nu)^2 = B(h\nu - E_g) \quad (1)$$

where E_g , h , α , ν , and B is a bandgap, Planck constant, absorption coefficient, light frequency, and a constant, respectively. The optical bandgap of the two samples was similar (2.44 eV).



6
Figure 1. XRD profile of Ag_3PO_4 and $\text{Ag}_3\text{PO}_4/\text{GO}$

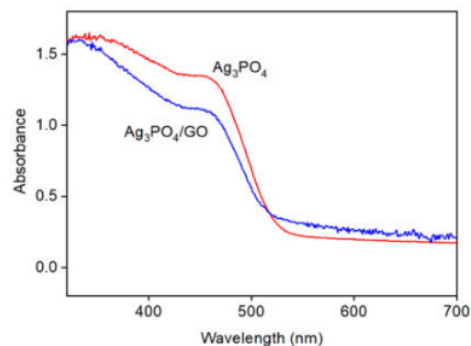


Figure 2. Absorption spectra of Ag_3PO_4 and $\text{Ag}_3\text{PO}_4/\text{GO}$ measured using DRS instrument

The diffraction peak of graphene oxide is not detected due to a very small GO impregnated on the surface of Ag_3PO_4 . The addition of GO did not change the structure, however, it can affect the intensity of diffraction. The higher intensity was observed in $\text{Ag}_3\text{PO}_4/\text{GO}$ suggested that the GO can improve the crystallinity. It is also found that the FWHM and 2 theta of $\text{Ag}_3\text{PO}_4/\text{GO}$ are higher than that of Ag_3PO_4 (Table 1). The three highest peaks at 33.358° , 36.624° , and 55.112° could be found in the sample of Ag_3PO_4 for (210), (211), and (320) diffractions, respectively. After incorporating the GO, the 2 theta shifted to 33.378° , 36.669° , and 55.130° . The distance of shift was found at 0.020° , 0.045° and 0.018° for (210), (211), and (320) diffractions, respectively. Among these shifts, the crystalline plane of {211} is more affected, suggesting that the defect might be higher created on this plane. This phenomenon occurred because the defect can affect the crystalline planes [20].

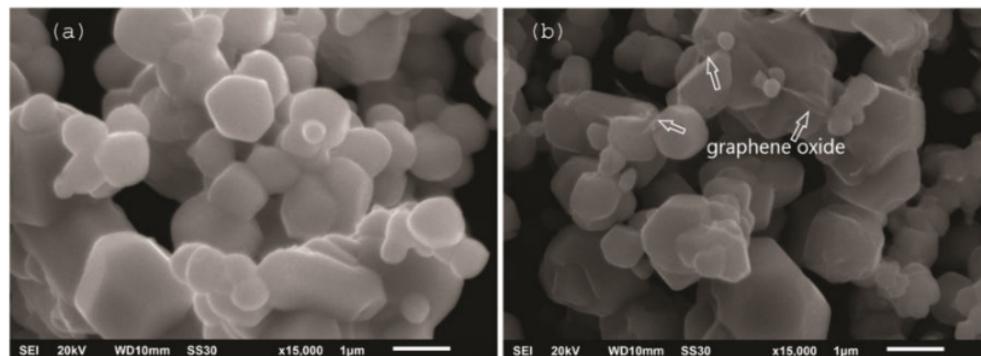
The morphology of Ag_3PO_4 and $\text{Ag}_3\text{PO}_4/\text{GO}$ were investigated, the results can be seen in figure 3a and figure 3b. The morphology of the two particles was not significantly changed after incorporating

GO. The crystal shape of samples is irregular ranging from 0.42 μm to 2 μm . A thin layer of graphene oxide was observed on the surface of $\text{Ag}_3\text{PO}_4/\text{GO}$. The GO forms a super thin layer that is strongly attached to the Ag_3PO_4 . Due to the hydroxyl and epoxide, a bond bridge between the GO and the cubic Ag_3PO_4 might form [21].

Table 1. Comparison of XRD data from the sample of Ag_3PO_4 and $\text{Ag}_3\text{PO}_4/\text{GO}$

Sample	2 θ	d (Å)	FWHM	Height (Counts)
Ag_3PO_4	33.358(3)	2.6839(2)	0.2043(19)	1270(36)
$\text{Ag}_3\text{PO}_4/\text{GO}$	33.378(3)	2.6823(3)	0.2174(17)	1520(33)

The elements of the sample were successfully analyzed using SEM-EDX and the atomic composition can be seen in table 2. A large impurity of carbon was formed in the precipitate of the samples. This impurity might be originated from the carbonate in the solution. Incorporation of GO on Ag_3PO_4 decrease the carbon impurity. Interestingly, the calcium ion from hydroxyapatite was not observed in SEM-EDX, indicating that the Ca^{2+} could not be precipitated and easily dissolved in water, whereas phosphate ion was successfully co-precipitated with silver forming Ag_3PO_4 .



9
Figure 3. SEM images of Ag_3PO_4 (a) and $\text{Ag}_3\text{PO}_4/\text{GO}$ (b)

Table 2. Atomic composition (%) from the SEM-EDX measurement of Ag_3PO_4 and $\text{Ag}_3\text{PO}_4/\text{GO}$.

Atom (%)	Ag_3PO_4	$\text{Ag}_3\text{PO}_4/\text{GO}$
Ag	10.35	18.78
P	3.61	6.64
O	36.78	46.40
C	46.43	23.01
Cu	0.52	1.07
Zn	0.35	0.89
Cd	0.82	1.28
Ar	1.14	1.94

Due to high carbon impurity, the precise investigation of the sample differences should be in the atomic ratio. The atomic ratios of P/Ag, O/Ag, and O/P in Ag_3PO_4 can be estimated at 0.35, 3.55, 10.2, respectively, whereas in the $\text{Ag}_3\text{PO}_4/\text{GO}$, they were 0.35, 2.47, and 6.99, respectively. The sample of Ag_3PO_4 and $\text{Ag}_3\text{PO}_4/\text{GO}$ has a similar atomic ratio of P/Ag but the atomic ratio of O/Ag and O/P in $\text{Ag}_3\text{PO}_4/\text{GO}$ is lower than that of Ag_3PO_4 , indicating that the incorporation of GO might influence the environment of co-precipitation. The lower ratio of O/P in $\text{Ag}_3\text{PO}_4/\text{GO}$ might be originated from the oxygen vacancy phenomenon.

The photocatalytic abilities of Ag_3PO_4 and $\text{Ag}_3\text{PO}_4/\text{GO}$ were investigated using RhB oxidation. The results can be seen in figure 4a. The pseudo-first-order reaction was utilized to investigate the profile of photocatalytic activity with the equation of $\ln(C_0/C_t)=kt$, C_t and C_0 are concentration at t time and initial concentration of photocatalytic reaction, k is the rate constant [16]. The pseudo-first-order reaction occurred in both Ag_3PO_4 and $\text{Ag}_3\text{PO}_4/\text{GO}$ with the rate constant of 0.455 min^{-1} and 0.670 min^{-1} , respectively. The $\text{Ag}_3\text{PO}_4/\text{GO}$ showed faster reaction activity (1.5 times faster than the Ag_3PO_4). Many results showed that the utilization of GO increased the adsorption [2,3], however, due to the low amount of GO impregnated on Ag_3PO_4 , the adsorption in the dark condition is not so high.

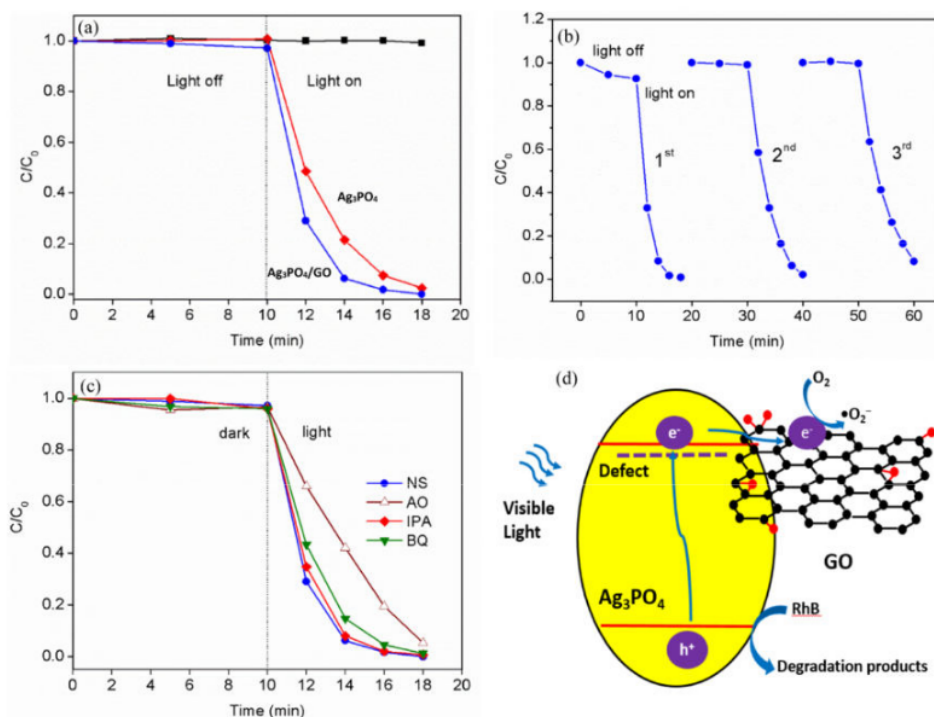


Figure 4. Photocatalytic activity of Ag_3PO_4 and $\text{Ag}_3\text{PO}_4/\text{GO}$ (a), Photocatalytic cycling of $\text{Ag}_3\text{PO}_4/\text{GO}$ (b), the effect of scavenger to photocatalytic in $\text{Ag}_3\text{PO}_4/\text{GO}$ (c) NS=no scavenger, AO=ammonium oxalate, IPA=isopropyl alcohol, BQ=benzoquinone, and the proposed mechanism of photocatalytic activity in $\text{Ag}_3\text{PO}_4/\text{GO}$ (d).

Recycled catalytic activity was also investigated (figure 4b). The catalytic activity decreased after cyclic reaction up to three times. The rates of photocatalytic reaction are 0.684 min^{-1} , 0.377 min^{-1} , and 0.243 min^{-1} for the reaction of 1st, 2nd, and 3rd, respectively. The decreased activity might be caused by the photoreduction of Ag^+ to Ag^0 . It suggested that although the photogenerated electrons can be highly separated through the GO, they have still reduced Ag^+ ions leading to photo-corrosion. Another reason is due to lower adsorption in the 2nd and 3rd reactions. The 1st reaction showed the adsorption in the dark condition, whereas 2nd and 3rd did not show the adsorption. This problem might be generated by the reaction 1st that can break the bond of GO from the Ag_3PO_4 leading to low adsorption on the surface.

The mechanisms of photocatalytic in $\text{Ag}_3\text{PO}_4/\text{GO}$ were studied using BQ (benzoquinone), AO (ammonium oxalate), and IPA (isopropyl alcohol) to scavenge the species of $\cdot\text{O}_2^-$, h^+ , and $\cdot\text{OH}$,

respectively[14]. The results were shown in figure 4c. The AO addition in reaction significantly quenched the photocatalytic reaction, showing that the reaction in the surface of $\text{Ag}_3\text{PO}_4/\text{GO}$ mostly runs via the h^+ . The mechanism runs in the following order: $h^+ \rightarrow \cdot\text{O}_2 \rightarrow \cdot\text{OH}$. The high role of h^+ in the mechanism might be generated by highly transferring a photogenerated electron to GO. When the $\text{Ag}_3\text{PO}_4/\text{GO}$ was exposed by the light, the electron in the VB of Ag_3PO_4 can be excited to the CB, producing a hole in the VB. The photogenerated electron in the CB transfers to GO, therefore the hole acts more efficiently to oxidize the RhB. The proposed mechanism in the surface reaction is shown in figure 4d.

The high role of the reaction mechanism is also through a superoxide radical ion. Because GO is a powerful electron acceptor, it can easily capture the photoexcited electrons. The photoexcited electron on the surface of GO could create a reduction reaction to produce a superoxide radical ion[22]. The GO on the surface of Ag_3PO_4 improved the separation of photoexcited electron and hole pair, leading to enhanced photocatalytic activity. The lattice defects generated by GO can serve as traps for electron trapping, which will also improve the separation of electrons and holes [6,23].

The role of $\cdot\text{OH}$ is not significant in the photocatalytic reaction mechanism. The $\cdot\text{OH}$ could be highly produced when water or hydroxyl ion (OH^-) adsorbed in the surface and reacted with hole producing $\cdot\text{OH}$. However, in this case, the adsorbates (RhB) might stronger be trapped by a hole under irradiation leading to decreased $\cdot\text{OH}$ formation on the surface of Ag_3PO_4 .

4. Conclusion

The co-precipitation of Ag_3PO_4 using the starting material of AgNO_3 , graphene oxide, and hydroxyapatite was successfully synthesized. The graphene oxide improves the crystallinity, decreases the impurity, and forms the defect in the surface of Ag_3PO_4 . The photocatalytic reaction of $\text{Ag}_3\text{PO}_4/\text{GO}$ runs faster than the Ag_3PO_4 . The enhanced photocatalytic activity was caused by improving the separation of photoexcited electrons and holes in the surface. The mechanism of the photocatalytic reaction was carried out by hole as a main role, and superoxide radical ion as a second role.

7 Acknowledgment

This research was partly financially supported by the Ministry of Research and Technology/National Research and Innovation Agency of Republic Indonesia.

6. References

- [1] Yu Z R, Li S N, Zang J, Zhang M, Gong L X, Song P, Zhao L, Zhang G D and Tang L C 2019 Enhanced mechanical property and flame resistance of graphene oxide nanocomposite paper modified with functionalized silica nanoparticles *Compos. Part B Eng.* **177** 107347
- [2] Ji B, Zhao W, Duan J, Fu L, Ma L, and Yang Z 2020 Immobilized $\text{Ag}_3\text{PO}_4/\text{GO}$ on 3D nickel foam and its photocatalytic degradation of norfloxacin antibiotic under visible light *RSC Adv.* **10** 4427–35
- [3] Deng M and Huang Y 2020 The phenomena and mechanism for the enhanced adsorption and photocatalytic decomposition of organic dyes with $\text{Ag}_3\text{PO}_4/\text{graphene oxide}$ aerogel composites *Ceram. Int.* **46** 2565–70
- [4] Ouyang K, Jiang N, Xue W, and Xie S 2020 Enhanced photocatalytic activities of visible light-responsive $\text{Ag}_3\text{PO}_4\text{-GO}$ photocatalysts for oxytetracycline hydrochloride degradation *Colloids Surfaces A Physicochem. Eng. Asp.* **604** 125312
- [5] Wu F, Zhou F, Zhu Z, Zhan S and He Q 2019 Enhanced photocatalytic activities of $\text{Ag}_3\text{PO}_4/\text{GO}$ in tetracycline degradation *Chem. Phys. Lett.* **724** 90–5
- [6] Khazae Z, Mahjoub A R, Cheshme Khavar A H, Srivastava V and Sillanpää M 2019 Synthesis of layered perovskite $\text{Ag}_2\text{F-Bi}_2\text{MoO}_6/\text{rGO}$: A surface plasmon resonance and oxygen vacancy promoted nanocomposite as a visible-light photocatalyst *J. Photochem. Photobiol. A*

- Chem.***379** 130–43
- [7] Zhu P, Duan M, Wang R, Xu J, Zou P and Jia H 2020 Facile synthesis of ZnO/GO/Ag₃PO₄ heterojunction photocatalyst with excellent photodegradation activity for tetracycline hydrochloride under visible light *Colloids Surfaces A Physicochem. Eng. Asp.***602** 125118
- [8] Wang J, Shen H, Dai X, Li C, Shi W and Yan Y 2018 Graphene oxide as solid-state electron mediator enhanced photocatalytic activities of GO-Ag₃PO₄/Bi₂O₃Z-scheme photocatalyst efficiently by visible-light driven *Mater. Technol.***33** 421–32
- [9] Wang H, Zou L, Shan Y and Wang X 2018 Ternary GO/Ag₃PO₄/AgBr composite as an efficient visible-light-driven photocatalyst *Mater. Res. Bull.***97** 189–94
- [10] Hong X, Wu X, Zhang Q, Xiao M, Yang G, Qiu M and Han G 2012 Hydroxyapatite supported Ag₃PO₄ nanoparticles with higher visible light photocatalytic activity *Appl. Surf. Sci.***258** 4801–5
- [11] Chang Q, Meng X, Hu S L, Zhang F and Yang J L 2017 Hydroxyapatite/N-doped carbon dots/Ag₃PO₄ composite for improved visible-light photocatalytic performance *RSC Adv.***7** 30191–8
- [12] Chai Y, Ding J, Wang L, Liu Q, Ren J and Dai W L 2015 Enormous enhancement in photocatalytic performance of Ag₃PO₄/HAp composite: A Z-scheme mechanism insight *Appl. Catal. B Environ.***179** 29–36
- [13] Li Y, Zhou H, Zhu G, Shao C, Pan H, Xu X and Tang R 2015 High efficient multifunctional Ag₃PO₄ loaded hydroxyapatite nanowires for water treatment *J. Hazard. Mater.***299** 379–87
- [14] Sulaeman U, Suhendar S, Diastuti H, Riapanitra A and Yin S 2018 Design of Ag₃PO₄ for highly enhanced photocatalyst using hydroxyapatite as a source of phosphate ion *Solid State Sci.***86** 1–5
- [15] Wang J D, Liu J K, Lu Y, Hong D J and Yang X H 2014 Catalytic performance of gold nanoparticles using different crystallinity HAP as carrier materials *Mater. Res. Bull.***55** 190–7
- [16] Sulaeman U, Hermawan D, Andreas R, Abdullah A Z and Yin S 2018 Native defects in silver orthophosphate and their effects on photocatalytic activity under visible light irradiation *Appl. Surf. Sci.***428** 1029–35
- [17] Cui X, Tian L, Xian X, Tang H and Yang X 2018 Solar photocatalytic water oxidation over Ag₃PO₄/g-C₃N₄ composite materials mediated by metallic Ag and graphene *Appl. Surf. Sci.***430** 108–15
- [18] Li L, Wang H, Zou L and Wang X 2015 Controllable synthesis, photocatalytic and electrocatalytic properties of CeO₂ nanocrystals *RSC Adv.***5** 41506–12
- [19] Li L, Zou L, Wang H and Wang X 2015 Converting Y(OH)₃ nanofiber bundles to YVO₄ polyhedrons for photodegradation of dye contaminants *Mater. Res. Bull.* **68** 276–82
- [20] Bi Y, Ouyang S, Umezawa N, Cao J and Ye J 2011 Facet effect of single-crystalline Ag₃PO₄ sub-microcrystals on photocatalytic properties *J. Am. Chem. Soc.* **133** 6490–6492
- [21] Mu C, Zhang Y, Cui W, Liang Y and Zhu Y 2017 Removal of bisphenol A over a separation free 3D Ag₃PO₄-graphene hydrogel via an adsorption-photocatalysis synergy *Appl. Catal. B Environ.***212** 41–9
- [22] Liu Z, Feng H, Xue S, Xie P, Li L, Hou X, Gong J, Wei X, Huang J and Wu D 2018 The triple-component Ag₃PO₄-CoFe₂O₄-GO synthesis and visible light photocatalytic performance *Appl. Surf. Sci.***458** 880–92
- [23] Du J, Ma S, Yan Y, Li K, Zhao F and Zhou J 2019 Corn-silk-templated synthesis of TiO₂ nanotube arrays with Ag₃PO₄ nanoparticles for efficient oxidation of organic pollutants and pathogenic bacteria under solar light *Colloids Surfaces A Physicochem. Eng. Asp.* **572** 237–49

The synthesis of Ag₃ PO₄ under graphene oxide and hydroxyapatite aqueous dispersion for enhanced photocatalytic activity

ORIGINALITY REPORT

13%

SIMILARITY INDEX

10%

INTERNET SOURCES

11%

PUBLICATIONS

5%

STUDENT PAPERS

PRIMARY SOURCES

1	www.coursehero.com Internet Source	2%
2	Uyi Sulaeman, Suhendar Suhendar, Hartiwi Diastuti, Anung Riapanitra, Shu Yin. "Design of Ag ₃ PO ₄ for highly enhanced photocatalyst using hydroxyapatite as a source of phosphate ion", Solid State Sciences, 2018 Publication	2%
3	eprints.covenantuniversity.edu.ng Internet Source	2%
4	ejournal2.undip.ac.id Internet Source	2%
5	eprints.untirta.ac.id Internet Source	1%
6	www.tandfonline.com Internet Source	1%
7	www.atlantis-press.com Internet Source	1%

8

Haoran Wang, Lei Zou, Yuchen Shan, Xiong Wang. "Ternary GO/Ag₃PO₄/AgBr composite as an efficient visible-light-driven photocatalyst", *Materials Research Bulletin*, 2018

Publication

1 %

9

Yuyu Bu, Zhuoyuan Chen. "Role of Polyaniline on the Photocatalytic Degradation and Stability Performance of the Polyaniline/Silver/Silver Phosphate Composite under Visible Light", *ACS Applied Materials & Interfaces*, 2014

Publication

1 %

10

Gang Liu, Hua Gui Yang, Jian Pan, Yong Qiang Yang, Gao Qing (Max) Lu, Hui-Ming Cheng. "Titanium Dioxide Crystals with Tailored Facets", *Chemical Reviews*, 2014

Publication

1 %

11

ar.kalasalilingam.ac.in

Internet Source

1 %

Exclude quotes

Off

Exclude matches

< 1%

Exclude bibliography

On